Chlorogenic acid enhances autophagy by upregulating lysosomal function to protect against SH-SY5Y cell injury induced by H_2O_2

LI-JUAN GAO[1,2*], YUAN DAI[2*], XIAO-QIONG LI[1,2], SHI MENG[1,2], ZHAN-QIONG ZHONG[1,3] and SHI-JUN XU[1,2]

[1]Institute of Meterial Medica Integration and Transformation for Brain Disorders; [2]School of Pharmacy; [3]School of Basic Medical Sciences, Chengdu University of Traditional Chinese Medicine, Chengdu, Sichuan 611137, P.R. China

Received November 4, 2019; Accepted August 11, 2020

DOI: 10.3892/etm.2021.9843

Abstract. Autophagy serves an important role in amyloid-β (Aβ) metabolism and τ processing and clearance in Alzheimer's disease. The progression of Aβ plaque accumulation and hyperphosphorylation of τ proteins are enhanced by oxidative stress. A hydrogen peroxide (H_2O_2) injury cell model was established using SH-SY5Y cells. Cells were randomly divided into normal, H_2O_2 and chlorogenic acid (5-caffeoylquinic acid; CGA) groups. The influence of CGA on cell viability was evaluated using a Cell Counting Kit-8 assay and cell death was assessed using Hoechst 33342 nuclear staining. Autophagy induction and fusion of autophagic vacuoles assays were performed using monodansylcadaverine staining. Additionally, SH-SY5Y cells expressing Ad-mCherry-green fluorescent protein-LC3B were established to detect autophagic flow. LysoTracker Red staining was used to evaluate lysosome function and LysoSensor™ Green staining assays were used to assess lysosomal acidification. The results demonstrated that CGA decreased the apoptosis rate, increased cell viability and improved cell morphology in H_2O_2-treated SH-SY5Y cells. Furthermore, CGA alleviated the accumulation of autophagic vacuoles, reduced the LC3BII/I ratio and decreased P62 levels, resulting in increased autophagic flux. Additionally, CGA upregulated lysosome acidity and increased the expression levels of cathepsin D. Importantly, these effects of CGA on H_2O_2-treated SH-SY5Y cells were mediated via the mTOR-transcription factor EB signaling pathway. These results indicated that CGA protected cells against H_2O_2-induced oxidative damage via the upregulation of autophagosomes, which promoted autophagocytic degradation and increased autophagic flux.

Correspondence to: Professor Shi-Jun Xu, Institute of Meterial Medica Integration and Transformation for Brain Disorders, Chengdu University of Traditional Chinese Medicine, 1166 Liutai Avenue, Chengdu, Sichuan 611137, P.R. China
E-mail: xushijun@cdutcm.edu.cn

Miss Zhan-Qiong Zhong, School of Basic Medical Sciences, Chengdu University of Traditional Chinese Medicine, 1166 Liutai Avenue, Chengdu, Sichuan 611137, P.R. China
E-mail: zhongzhanqiong@cdutcm.edu.cn

*Contributed equally

Key words: Alzheimer's disease, chlorogenic acid, autophagy, transcription factor EB, lysosomal

Introduction

Alzheimer's disease (AD) is a progressive neurodegenerative disease characterized by memory loss, cognitive dysfunction, personality changes and decreased mobility (1). Furthermore, AD is pathologically characterized by senile plaques (SP) and neurofibrillary tangles (1). According to a 2019 report by the Alzheimer's Association, the risk of developing AD has increased to 1:10 for individuals older than 65 years and is as high as 1:2 among individuals older than 85 years in USA (2). Therefore, effective treatments and controlling the pathological processes underlying AD are of great concern in the medical field.

The pathogenesis of AD is complex and there are numerous hypotheses regarding its occurrence, including neuroinflammation, cholinergic dysfunction, metabolic alterations, amyloid-β (Aβ) peptide accumulation and abnormalities in τ protein metabolism (3-5). Although these hypotheses are controversial, the accumulation of Aβ is one of the major theories recognized by researchers (6). According to the Aβ cascade hypothesis, mutations in the amyloid precursor protein (APP), presenilin-1 (PS-1) and PS-2 upregulate Aβ secretion, leading to the accumulation of Aβ, which forms small molecule oligomers that are further aggregated into fibers and deposited to form extracellular SPs (7). Aβ plaques create an environment that allows for the rapid induction of pathological τ aggregates from endogenous τ and may enhance or sustain τ pathologies through additional mechanisms, including intracellular protein degradation impairment (8). Furthermore, Aβ plaques induce oxidative stress and mediate damage to numerous biological macromolecules, including proteins, nucleic acids and lipids, resulting in changes of neuronal structure and function, and potential neuronal loss (9). A previous study has indicated an association between oxidative stress and protein aggregation processes, which are involved in the development of proteinopathies (10). Therefore, oxidative

stress can be considered either causative or consecutive in regard to protein aggregation (11). Furthermore, recent studies have demonstrated that medications used to successfully treat AD-like symptoms act by modulating oxidative stress (12,13).

Autophagy is involved in numerous diseases, including cancer, diabetes and neurodegenerative disorders (14). Autophagy consists of a dynamic pathway, including the formation of surrounding membranes and the degradation of diverse cellular components, such as organelles and protein aggregates (15). Additionally, autophagy serves an important role in Aβ metabolism and τ processing and clearance (16). Furthermore, autophagy contributes to endoplasmic reticulum stress and mitophagy in relation to AD pathology (17,18).

Chlorogenic acid (5-caffeoylquinic acid; CGA) is a polyphenolic substance that is widely found in the human diet (19). CGA has various pharmacologic actions, including antioxidant, anti-inflammatory and anticarcinogenic activities, that exert hypoglycemic and hypolipidemic effects (20). A number of studies have indicated that dietary consumption of CGA reduces the risk of developing neurodegenerative diseases (21,22). An *in vitro* biological study revealed that CGA has an enhanced inhibitory effect on Aβ40 aggregation and protects PC12 cells from Aβ-aggregation-induced cell death (23). Additionally, a previous study demonstrated the neuroprotective effects of CGA and its major metabolites in primary cultures of rat cerebellar granule neurons (24). Furthermore, numerous studies have reported that CGA reduces the risk of neurodegenerative diseases (21,22); however, the mechanism by which CGA confers this protective effect remains unclear. To investigate the underlying mechanism, the present study employed a hydrogen peroxide (H_2O_2)-induced SH-SY5Y cell model and investigated whether CGA regulated autophagic flow and lysosomal function via the mTOR/transcription factor EB (TFEB) pathway to protect against H_2O_2-induced cell damage.

Materials and methods

Cell model and CGA treatment. SH-SY5Y human neuroblastoma cells were purchased from Shanghai Zhong Qiao Xin Zhou Biotechnology Co., Ltd. (cat. no. 20161116-02) and were authenticated by a short tandem repeat profiling service provided by American Type Culture Collection. CGA (purity, ≥98%; assessed by high performance liquid chromatography) was purchased from Baoji Herbest Bio-Tech Co., Ltd. The details were as follows: Instrument: Spd-16 High performance liquid chromatography (Shimadzu Corporation); chromatographic column, Sepax Bio-C18 [Yuexu Technology (Shanghai) Co., Ltd.; 4.6x250 mm; 5 μl]; temperature, 30˚C; injection volume, 20 μl; mobile phase, acetonitrile-0.4% acetic acid aqueous solution; velocity of flow: 1.0 ml/min; and detection wavelength, 350 nm. H_2O_2 (34.01 g/mol) was purchased from Sigma-Aldrich; Merck KGaA.

The cell model was established as previously described (25). Briefly, SH-SY5Y cells were cultured in DMEM (Gibco; Thermo Fisher Scientific, Inc.) supplemented with 10% FBS (Zhejiang Tianhang Bio Polytron Technologies Inc.) and 1% penicillin/streptomycin (Gibco; Thermo Fisher Scientific, Inc.) and incubated at 37˚C in a humidified atmosphere containing 5% CO_2 (3111 CO_2 incubator; Thermo Fisher Scientific, Inc.).

Cells in the logarithmic growth phase were selected and digested with 0.25% trypsin (Gibco; Thermo Fisher Scientific, Inc.). Subsequently, cells were seeded into 96-well plates (seeding density, $3x10^4$ cells/ml) for 16 h. To determine the optimal concentration and duration of H_2O_2 treatment to elicit toxic effects on SH-SY5Y cells, cells were treated with 50, 100, 200, 400, 500, 600, 700 or 800 μM H_2O_2 for 4, 8, 12 or 48 h. After 12 h of plating, the medium was replaced with CGA (100, 50, 25, 12.5, 6.25 and 3.125 μM) in the CGA groups or fresh DMEM in the normal and model groups. These cells were incubated for an additional 24 h prior to analyses.

Cell viability assessment using a Cell Counting Kit-8 (CCK-8) assay. Cell viability was measured using CCK-8 assays according to the manufacturer's protocol. Briefly, cells were treated with different concentrations of H_2O_2 and viability was measured at 12, 24 and 36 h. Cells were treated with 10 μl CCK-8 reagent (cat. no. JE914; Dojindo Molecular Technologies, Inc.) for 2 h at 37˚C. Following this, optical density (OD) values were measured at a wavelength of 450 nm using an automatic microplate reader (Thermo Fisher Scientific, Inc.). The SH-SY5Y cells were treated with different concentrations of CGA (0, 100, 200, 300, 400, 500, 600, 700 and 800 μM) for 12, 24 and 36 h to determine the optimal concentration, and cell viability was detected using the CCK-8 assay. Cell viability (%) was calculated as follows: $OD_{\text{value of the administration well}} - OD_{\text{value of the zero well}}/OD_{\text{value of the normal well}} - OD_{\text{value of the zero well}}$. Morphologic changes were observed using phase-contrast microscopy (x400), and analysis of the length of cell processes and numbers of SH-SY5Y cells were analyzed using Image-Pro Plus software (version 6.0; Media Cybernetics, Inc.).

Monodansylcadaverine (MDC) and Hoechst fluorescence staining. MDC (Sigma-Aldrich; Merck KGaA) is a lysosomotropic compound used for the identification of autophagic vesicles via fluorescence microscopy and for the assessment of autophagy induction via the accumulation of MDC-labeled vacuoles (26). Hoechst staining was used to test for cell apoptosis. CGA (50, 25, 12.5 and 6.25 μM) and/or H_2O_2 (500 μM) was added to each well at 37˚C. After 24 h, cells ($1x10^6$/well) were washed twice with PBS and treated with 500 μl MDC solution (25 μM) or Hoechst solution (50 μM) and incubated for 30 min at 37˚C. Fluorescence images were captured using an inverted fluorescence microscope (DMI3000; Leica Microsystems GmbH) and analyzed using Image-Pro Plus software (version 6.0; Media Cybernetics, Inc.).

Autophagic flow test. mCherry-green fluorescent protein (GFP)-LC3 adenoviruses (cat. no. 030217170302; Beyotime Institute of Biotechnology) were infected into SH-SY5Y cells, according to the manufacturer's protocol. SH-SY5Y cells were inoculated into 24-well plates ($2.5x10^5$/well) and cultured for 24 h at 37˚C. Subsequently, the culture medium was removed and a virus solution at MOI=5 was added. Cells that were not exposed to the virus served as the control group. Cells were cultured for 12 h at 37˚C with 5% CO_2. After 24 h of treatment with CGA (50 μM) and/or H_2O_2 (500 μM), mean fluorescence intensities were measured using Image-Pro Plus software.

Western blotting. The primary antibodies used in the present study were as follows: Anti-rabbit-sequestosome 1 (SQSTM1)/p62 (1:1,000; Cell Signaling Technology, Inc.), anti-rabbit-Lamin A/C (1:1,000; Cell Signaling Technology, Inc.), anti-rabbit-phosphorylated-mTOR Ser 2448 (P-mTOR; 1:1,000; Cell Signaling Technology, Inc.), anti-rabbit-TFEB (1:1,000; Cell Signaling Technology, Inc.), anti-rabbit-mTOR (1:1,000; Cell Signaling Technology, Inc.), anti-rabbit-LC3B (1:500; Cell Signaling Technology, Inc.), anti-rabbit-Beclin 1 (1:500; BIOSS), anti-rabbit-autophagy protein 5 (Atg5)/autophagy related 5 (1:1,000; BIOSS), anti-rabbit GAPDH (1:5,000; Wuhan Servicebio Technology Co., Ltd.), anti-rabbit-cathepsin D (CTSD; 1:500; Beyotime Institute of Biotechnology), anti-rabbit-Bcl-2 (1:500; Wuhan Sanying Biotechnology), anti-rabbit-Bax (1:500; Wuhan Sanying Biotechnology Co., Ltd.). Cells were washed with PBS and subjected to lysis at 4˚C in RIPA lysis buffer (Servicebio Technology Co., Ltd.) supplemented with phenyl methylsulfonyl fluoride [Hangzhou Multi Sciences (Lianke) Biotech Co., Ltd.], phosphatase inhibitors (Boster Biological Technology) at a ratio of 100:1:1 and a cocktail of protease inhibitors [Hangzhou Multi Sciences (Lianke) Biotech Co., Ltd.]. Cell suspensions were centrifuged at 800 x g for 10 min at 4˚C and protein concentrations were quantified using a BCA kit (Sichuan Mike Biological Technology Co., Ltd.). Protein extracts (30 μg/lane) were separated and fractionated via 8-15% SDS-PAGE and transferred to a PVDF membrane (Merck KGaA). The membranes were blocked with 5% BSA (Guangzhou Saiguo Biotech Co., Ltd.) for 90 min at room temperature. Cells were incubated with primary antibodies overnight at 4˚C. After washing with TBS with 0.1% Tween-20, membranes were incubated with horseradish peroxidase-conjugated goat anti-rabbit secondary antibodies (1:5,000; BIOSS) for 2 h at room temperature. The best blocking reagent was 5% BSA at 90 min. Following washing, bands were visualized using an ECL kit (Beijing 4A Biotech Co., Ltd.). Quantity One software (v4.6.6; Bio-Rad Laboratories, Inc.) was used for quantification.

LysoTracker Red and LysoSensor™ Green staining. Lysosomal staining was performed using LysoTracker Red and LysoSensor Green staining assays in order to assess lysosomal acidification. Following 16 h of treatment with CGA (50 μM) at 37˚C, Earle's Balanced Salt Solution (EBSS; cat. no. 354655A; incubation, 30 min; Beyotime Institute of Biotechnology), chloroquine (CQ; 25 μM; incubation, 2 h; cat. no. J0102A; Dalian Meilun Biology Technology Co., Ltd.) and H_2O_2 (500 μM; incubation, 12 h) were added. Cells ($2.5x10^5$/well) were subsequently incubated with LysoTracker Red (5 μl) and LysoSensor Green (10 μl) for 30 min at 37˚C, washed with PBS and examined using fluorescence microscopy (Leica Microsystems GmbH). The mean fluorescence intensity was measured using Image-Pro Plus software (version 6.0; Media Cybernetics, Inc.).

Statistical analysis. Statistical analysis was performed using SPSS software (version 21.0; IBM Corp.). Quantitative data are presented as the mean ± SD. All experiments were repeated at least three times Non-parametric tests were used for data that were not normally distributed. Comparisons among different groups were performed using one-way ANOVA. If the datasets contained more than three groups, Tukey's multiple comparison analysis was used. $P<0.05$ was considered to indicate a statistically significant difference.

Results

Effect of CGA on SH-SY5Y cells. SH-SY5Y cells were treated with different concentrations of H_2O_2 to determine the optimal concentration for subsequent experiments, as assessed by CCK-8 assays. Different concentrations of H_2O_2 (100-800 μM) affected cells differently at 12 and 24 h compared with the normal group (Fig. 1A). Treatment with H_2O_2 decreased cell viability in a dose- and time-dependent manner, and the IC_{50} of 500 μM H_2O_2 regarding cell injury at 24 h was 973.90 μM. The cell viability was 69.25±3.17% following treatment with 500 μM H_2O_2 for 24 h. Based on the results of this experiment and previous studies, 500 μM H_2O_2 and 24 h were selected as the optimal damage conditions for subsequent experiments (27,28).

According to previous study, CGA has a protective effect induced by H_2O_2 (29). However, CGA treatment decreased cell viability and exhibited drug toxicity at concentrations of 50-400 μM at 12-36 h (Fig. 1B). Therefore, 6.25-50 μM was regarded as the optimum concentration range for CGA treatment in the present study.

Neuroprotective effect of CGA on SH-SY5Y cells injured by H_2O_2. To investigate the effects of CGA on SH-SY5Y cells injured by H_2O_2, four concentrations of CGA (50, 25, 12.5 and 6.25 μM) were used. The morphology of the cells was altered following 24 h of incubation with CGA (Fig. 1C). Data revealed that the length of cell processes significantly reduced in the H_2O_2 group, luckily, it could be rescue by CGA, CGA concentrations of 50 and 12.5 μM ameliorated the morphological alterations (length of cell processes) of the cell model (Fig. 1D). Similarly, the numbers and viability of the SH-SY5Y cells were rescued by all concentrations of CGA (Fig. 1E and G).

Cell apoptosis was assessed with Hoechst staining and the average cell apoptosis rate was significantly decreased in each CGA treatment group compared with the H_2O_2 treatment group (Fig. 1F and H). The changes of Bax and Bcl-2 protein expression may play an important role in cell apoptosis (30). Therefore, the results demonstrated that CGA upregulated Bcl-2 expression and downregulated Bax expression to inhibit cell apoptosis (Fig. 1I). It has been suggested that the Bax/Bcl-2 ratio may be more important than either protein alone in determining apoptosis (31). These results indicated that CGA alleviated the morphological damage and effectively reduced apoptosis in H_2O_2-treated SH-SY5Y cells.

Effect of CGA on autophagic flux in SH-SY5Y cells treated with H_2O_2. The effects of CGA on the accumulation of autophagic vacuoles in SH-SY5Y cells injured by H_2O_2 were assessed. H_2O_2 treatment increased the average fluorescence intensity of MDC in a time-dependent manner when compared with the control group (Fig. 2A and B). Furthermore, the different concentrations of CGA significantly reduced the average fluorescence intensity of MDC in the cell model at 12 and 24 h (Fig. 2A and B).

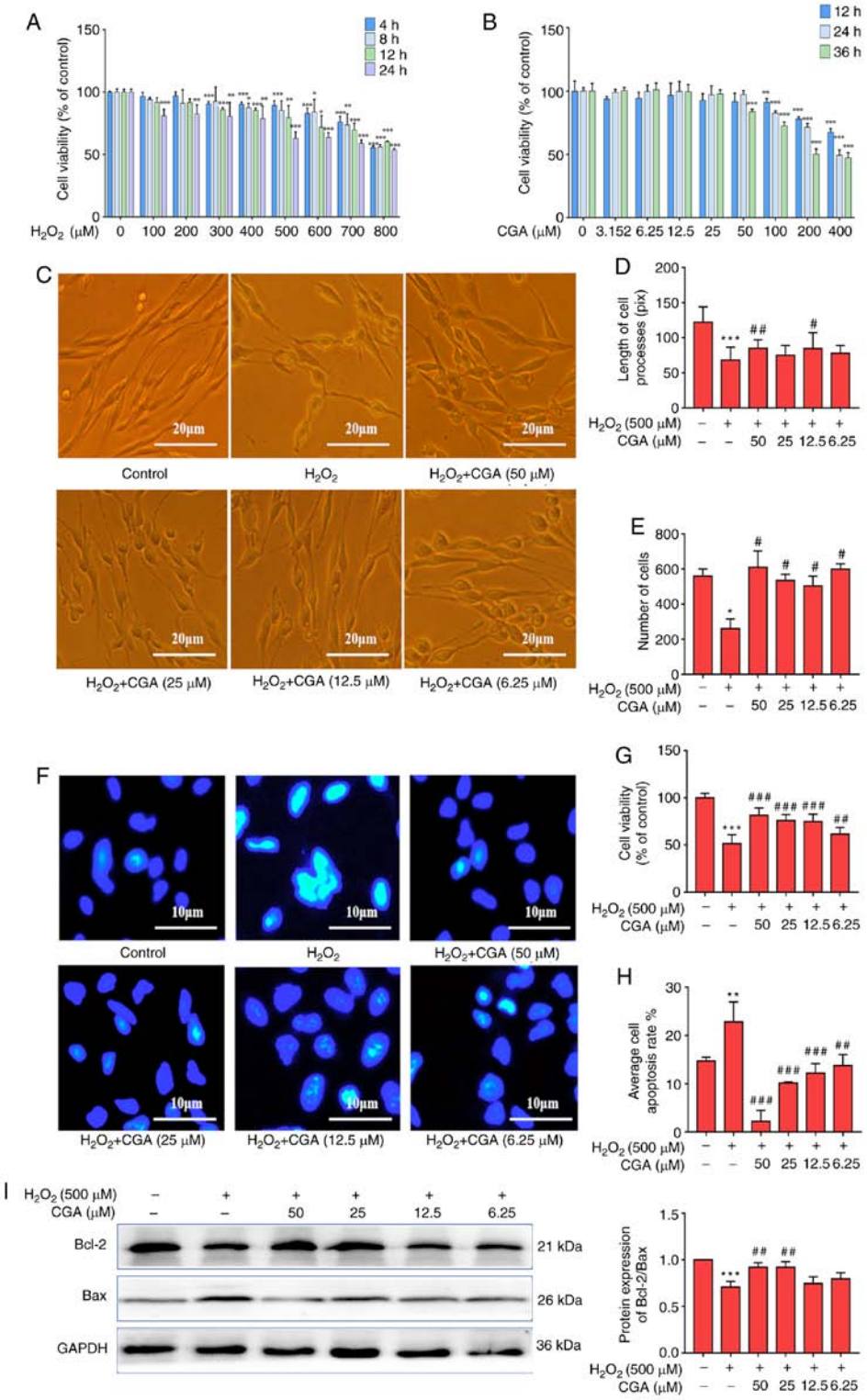

Figure 1. Neuroprotective effects of CGA on SH-SY5Y cells injured by H_2O_2. (A) Cell viability of SH-SY5Y cells damaged by different concentrations of H_2O_2 at 4, 8, 12 and 24 h. (B) Cell viability of SH-SY5Y cells following treatment with different concentrations of CGA for 12, 24 and 36 h. (C) Morphology of SH-SY5Y cells in the different groups. Scale bar, 20 μm. (D) Concentrations of 50 and 12.5 μM CGA restored the morphology of SH-SY5Y cells damaged by H_2O_2 for 24 h. (E) Numbers of SH-SY5Y cells were rescued by different concentrations of CGA. (F) Hoechst staining of SH-SY5Y cells in each group. Scale bar, 10 μm. (G) Cell viability of SH-SY5Y cells was significantly increased by different concentrations of CGA compared with control group. (H) Average cell apoptosis rate was significantly decreased in each CGA group. (I) Representative western blotting images of Bcl-2 and Bax expression in SH-SY5Y cells (left panel). GAPDH was used as the loading control. Relative optical density values of Bcl-2/Bax (right panel). *P<0.05, **P<0.01 and ***P<0.001 vs. control group. $^{\#}$P<0.05, $^{\#\#}$P<0.01 and $^{\#\#\#}$P<0.001 vs. H_2O_2 treatment group. CGA, chlorogenic acid; H_2O_2, hydrogen peroxide; Bcl-2, B-cell lymphoma 2; Bax, Bcl-2 associated X.

Autophagic flux is a dynamic process and includes the formation of autophagosomes, fusion of autophagosomes with lysosomes and cargo degradation. Atg5 and Beclin-1 are involved in the formation of autophagosomes (32) and the

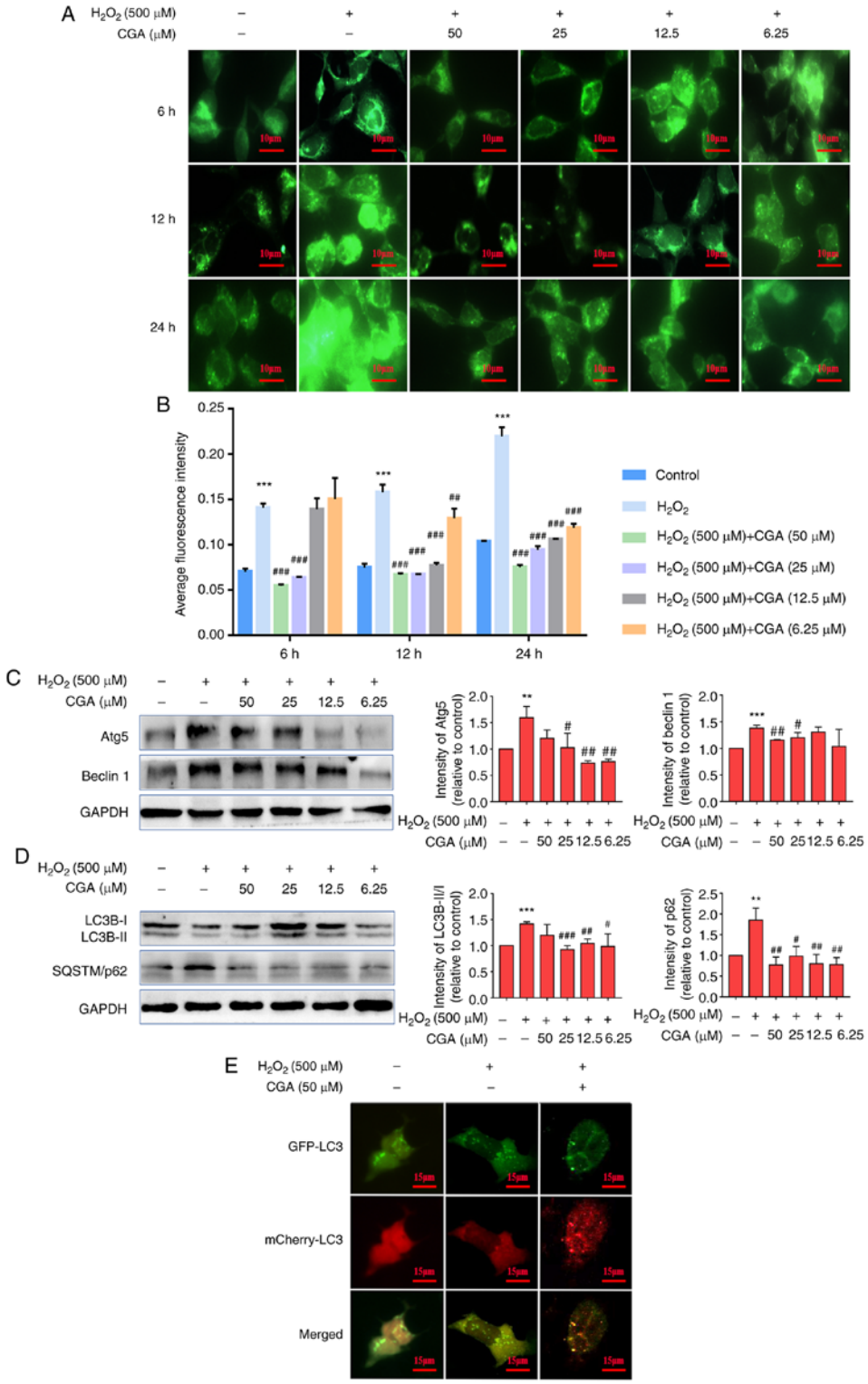

Figure 2. Effects of CGA on autophagic flux in SH-SY5Y cells injured by H_2O_2. (A) Effects of CGA on autophagic vacuole accumulation in SH-SY5Y cells injured by H_2O_2. Scale bar, 10 μm. (B) CGA treatments significantly reduced the average fluorescence intensity of monodansylcadaverine at 6 (25 and 50 μM), 12 and 24 h compared with the H_2O_2 group. (C) Intensity of Beclin-1 bands in SH-SY5Y cells was decreased following incubation with 50 or 25 μM CGA compared with the H_2O_2 group. Additionally, the intensity of Atg5 bands was decreased in the 25, 12.5 and 6.25 μM CGA groups. Beclin-1 and Atg5 levels were normalized to GAPHD. (D) Intensity of LC3B-II/I bands in the SH-SY5Y cells was decreased following incubation with 25, 12.5 and 6.25 μM CGA compared with the H_2O_2 group. Additionally, the intensity of the SQSTM/p62 bands was decreased in each CGA group. LC3-II/I and p62 levels were normalized to GAPHD. (E) mCherry-GFP-LC3 adenovirus transfection was used to detect the effect of CGA on SH-SY5Y cells. mCherry-GFP-LC3 specifically labels autophagosomes. Scale bar, 15 μm. **P<0.01 and ***P<0.001 vs. control group; $^{\#}$P<0.05, $^{\#\#}$P<0.01 and $^{\#\#\#}$P<0.001 vs. H_2O_2 treatment group. CGA, chlorogenic acid; H_2O_2, hydrogen peroxide; Atg5, autophagy protein 5; SQSTM, sequestosome 1; GFP, green fluorescent protein.

results indicated that H_2O_2 increased Atg5 and Beclin-1 levels, which likely promoted an enhancement of autophagosome formation. To further characterize the effects of CGA on autophagic flux in the SH-SY5Y cell model, autophagy-

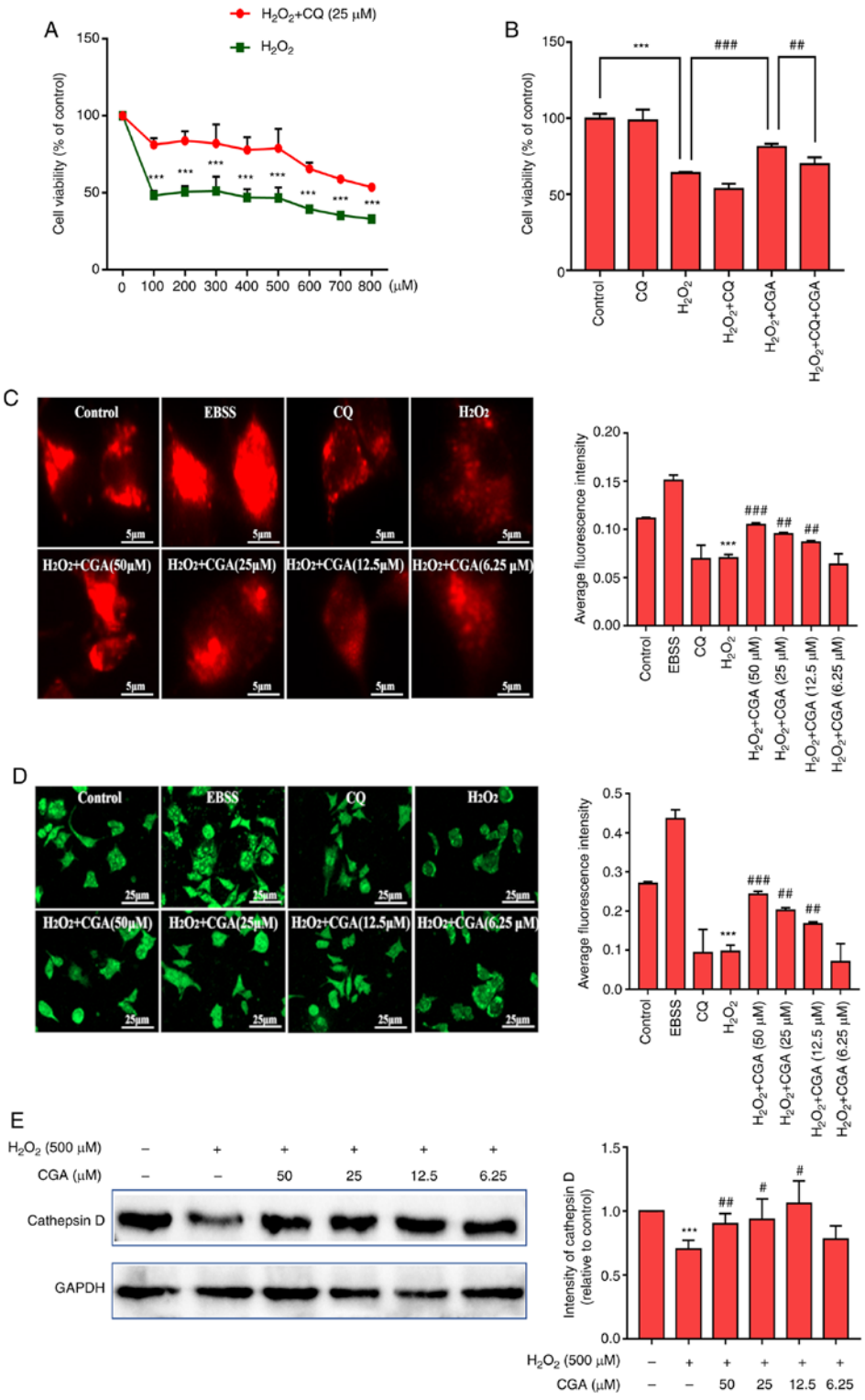

Figure 3. Effect of CGA on lysosome function in SH-SY5Y cells injured by H_2O_2. (A) CQ pretreatment prevented damage to SH-SY5Y cells as the cell viability of SH-SY5Y cells was significantly decreased in the H_2O_2 + CQ group. ***P<0.001 vs. H_2O_2 group. (B) Cell viability of SH-SY5Y cells was reduced by H_2O_2 treatment; however, cell viability was rescued by CGA treatment. However, cell viability was lower in the H_2O_2 + CQ + CGA group compared with the H_2O_2 + CGA group. ***P<0.001, $^{\#\#}$P<0.05 and $^{\#\#\#}$P<0.01, as indicated. (C) LysoTracker Red was used to specifically label intracellular lysosomes. Scale bar, 5 μm. ***P<0.001 vs. control group; $^{\#\#}$P<0.01 and $^{\#\#\#}$P<0.001 vs. H_2O_2 treatment group. (D) Lysosomes were labeled with LysoSensor Green and observed by fluorescence microscopy. Scale bar, 25 μm. ***P<0.001 vs. control group; $^{\#\#}$P<0.01 and $^{\#\#\#}$P<0.001 vs. H_2O_2 treatment group. (E) Representative western blotting images of CTSD in SH-SY5Y cells (left panel). ***P<0.001 vs. control group; $^{\#}$P<0.05 and $^{\#\#}$P<0.01 vs. H_2O_2 treatment group. GAPDH was used as the internal control. Relative optical density values of CTSD in the experimental groups (right panel). CGA, chlorogenic acid; H_2O_2, hydrogen peroxide; CQ, chloroquine; CTSD, cathepsin D; EBSS, Earle's Balanced Salt Solution.

associated proteins were assessed in each group. Western blotting demonstrated that the expression levels of Beclin-1 in the 50 and 25 μM CGA groups and Atg5 in the 25, 12.5 and 6.25 μM CGA groups were significantly downregulated

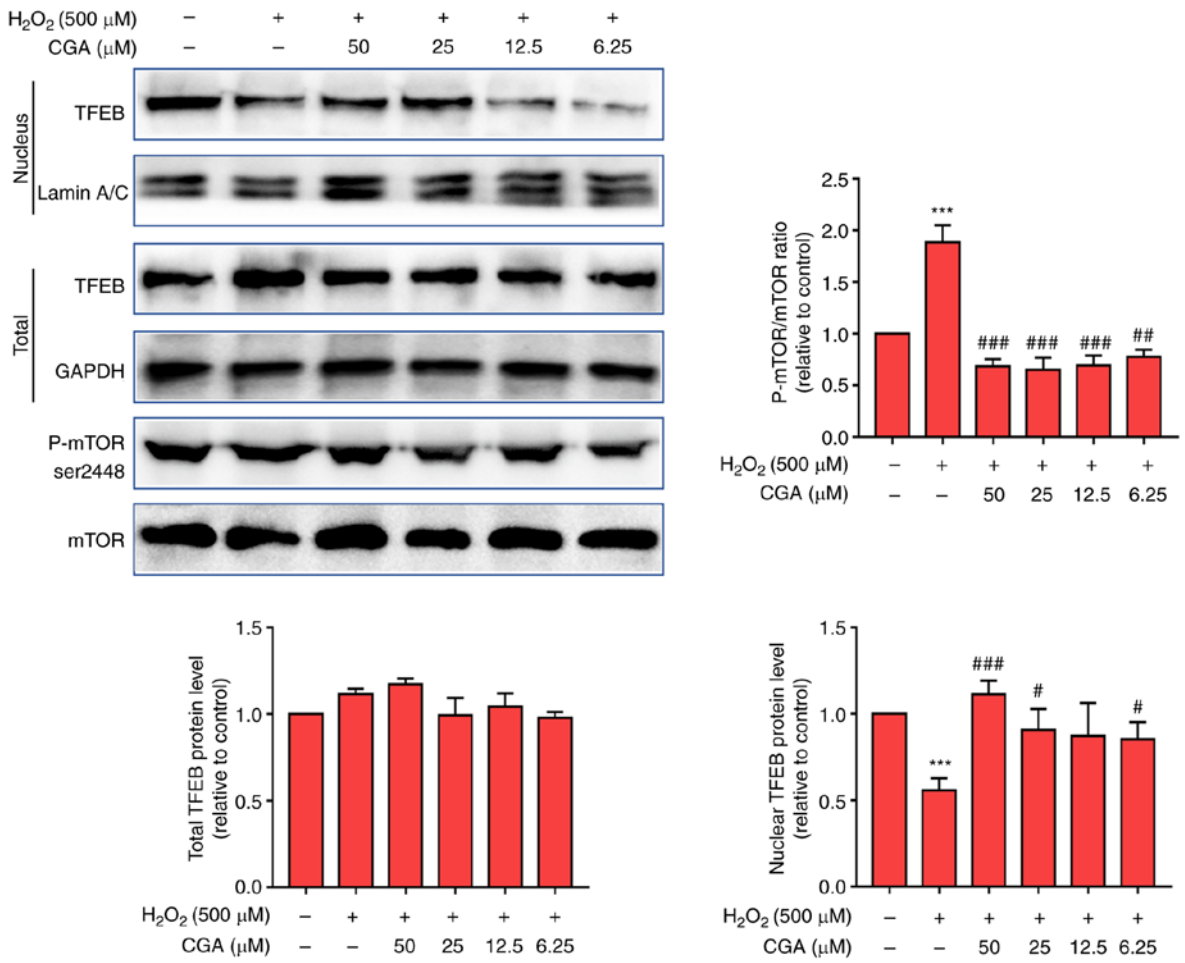

Figure 4. Effect of CGA on the mTOR-TFEB signaling pathway in H_2O_2-treated SH-SY5Y cells. Nuclear TFEB expression was increased in the 50, 25 and 6.25 μM CGA groups. However, total TFEB levels were not significantly different among groups. The ratio of P-mTOR/mTOR TFEB was significantly reduced in all CGA groups. TFEB and P-mTOR/mTOR were normalized to GAPHD. ***P<0.001 vs. control group. $^{\#}$P<0.05, $^{\#\#}$P<0.01 and $^{\#\#\#}$P<0.001 vs. H_2O_2 treatment group. CGA, chlorogenic acid; H_2O_2, hydrogen peroxide; TFEB, transcription factor EB; P-, phosphorylated; ser, serine.

(Fig. 2C). These data indicated that CGA inhibition of autophagosome production may occur via the downregulation of Beclin-1 and Atg5 expression.

To determine whether CGA had any effect on H_2O_2-mediated autophagy activation, western blotting was performed. The results indicated that the intensity of LC3B-II/I bands in the SH-SY5Y cell model was decreased in the 25, 12.5 and 6.25 μM CGA groups compared with the H_2O_2 treatment group. P62/SQSTM1 is an autophagy-selective substrate complex and LC3B-II is localized on the inner membrane to form the complex (33). The expression levels of P62/SQSTM1 were decreased in each CGA treatment group (Fig. 2D). Therefore, these results suggested that CGA increased autophagic flux by reducing the levels of LC3-II/I and P62/SQSTM1.

SH-SY5Y cells successfully transfected with mCherry-GFP-LC3 were used as vectors to investigate the effect of CGA on autophagic flow. When autophagy is activated, the fluorescent GFP signal enters the lysosome. However, during autophagy flux, lysosomes fuse with autophagosomes, and the green (GFP) fluorescence is quenched by the acidic microenvironment whereas the mCherry signal remains stable (34). After entering the lysosome, the mCherry signal can still be observed (34). The co-localization of GFP and mCherry (observed as yellow fluorescence) represents the blockage of autophagic flow. Compared with the H_2O_2 treatment group, treatment with CGA reduced the occurrence of mCherry$^+$ GFP$^+$ (yellow) spots induced by H_2O_2 and increased the occurrence of mCherry$^+$ GFP$^-$ (red) spots (Fig. 2E).

Effect of CGA on lysosome function in SH-SY5Y cells injured by H_2O_2. To investigate how CGA activity may affect autophagy, lysosome function in the SH-SY5Y cell model was assessed. CQ is a lysosomal blocker that blocks the autophagy-lysosomal pathway (ALP) by alkalizing the acidic environment of lysosome and inhibiting the degradation of lysosomes (35). Following 25 μM CQ pretreatment for 2 h to inhibit lysosome activity, the results indicated that CQ successfully reversed the decreased cell viability conferred by H_2O_2 treatment (Fig. 3A). These results indicated that H_2O_2 reduced cell viability, and CGA significantly relieved the damage caused by H_2O_2 in SH-SY5Y cells. However, CQ had an antagonistic effect on the anti-H_2O_2 effects of CGA in regard to cytotoxicity (Fig. 3B).

Following this, the effects of CGA on the lysosomal acidity of H_2O_2-treated SH-SY5Y cells were investigated. LysoTracker

Red specifically labels intracellular lysosomes and these are presented as red fluorescent spots under a fluorescence microscope. LysoSensor Green exhibits a pH-dependent increase in fluorescence intensity following acidification, which is used to detect the effect of CGA on the lysosomes. EBSS is a balanced salt solution that induces autophagosome formation via starvation while rapidly upregulating the acidic environment of the lysosomes and, therefore, promoting lysosomal degradation and enhancing the ALP (36). H_2O_2 treatment significantly decreased the average fluorescence intensity of LysoTracker Red (Fig. 3C). Compared with the H_2O_2 treatment group, the 50, 25 and 12.5 μM CGA groups exhibited significant upregulation of the mean fluorescence intensity of LysoTracker Red induced by H_2O_2. The acidic intracellular compartments (lysosomes) in SH-SY5Y cells were measured using LysoSensor Green. H_2O_2 (500 μM) exposure significantly reduced the fluorescence signal compared with the control group (Fig. 3D), indicating a H_2O_2-mediated reduction of intracellular acidic components. Furthermore, treatment with CGA significantly increased LysoSensor Green fluorescence compared with the H_2O_2 treatment group. Finally, the expression levels of CTSD in the different CGA groups were determined. These data revealed that the levels of CTSD were significantly enhanced in the 50, 25 and 12.5 μM CGA + H_2O_2 groups compared with the H_2O_2 treatment group (Fig. 3E).

Effect of CGA on the mTOR-TFEB signaling pathway in SH-SY5Y cells treated with H_2O_2. Western blotting was used to determine total protein and TFEB levels in cell nuclei. The results indicated that H_2O_2 had no significant effect on the overall levels of TFEB in cells (Fig. 4). However, H_2O_2 significantly decreased the levels of nuclear TFEB and increased the ratio of P-mTOR/mTOR compared with the normal group. Furthermore, CGA treatment (50, 25 and 6.25 μM) significantly increased the levels of nuclear TFEB and decreased the ratio of P-mTOR/mTOR compared with the H_2O_2 treatment group.

Discussion

A previous study has reported that natural compounds reduce the risk of developing neurodegenerative conditions, including vitamins A, C, and E and β-carotene (37). The present study provided additional evidence for the pivotal role of CGA in AD pathogenesis. CGA attenuated cell injury and apoptosis, reduced autophagy overactivation, increased autophagic flux and enhanced lysosomal function in SH-SY5Y cells injured by H_2O_2. Additionally, the results demonstrated that CGA may inhibit excessive autophagy by regulating the mTOR-TFEB signaling pathway and decreasing TFEB nuclear translocation.

AD is a neurodegenerative disorder with no known cure (1). The progression of Aβ plaque accumulation and hyperphosphorylation of τ proteins are enhanced by oxidative stress (38). The risk of AD increases significantly with age and, based on the hypotheses proposed to explain the causes of aging and AD, it has been reported that oxidative stress serves a central role in this occurrence (37). A previous study has indicated that brain tissues of patients with AD are exposed to oxidative stress during the development of the disease (39). Over time, oxidative stress contributes to a range of aging-related degenerative diseases, including cancer, diabetes, macular degeneration and AD (37). Furthermore, oxidative stress is one of the main causes of neuronal degeneration and loss-of-function in patients with AD and it can interact with β-amyloid peptides and activate signaling pathways to promote the occurrence and progression of AD (37). Neuroblastoma cell lines, including SH-SY5Y, are the most frequently utilized models in neurodegenerative studies and their use has advanced the understanding of the pathology of neurodegeneration over the past few decades (40).

CGA is a phenylpropanoid compound produced in plants via the shikimic acid pathway during aerobic respiration (22). Polyphenols are secondary plant metabolites, comprising several antioxidant compounds and are generally considered to be involved in the defense against numerous chronic human diseases, including prostate cancer among others, cardiovascular diseases, diabetes mellitus and neurodegenerative diseases, such as Alzheimer's and Parkinson's disease (41). CGA is a polyphenolic substance widely found in the human diet (22). CGA has various pharmacologic actions, including antioxidant, anti-inflammatory and anticarcinogenic functions, and exerts hypoglycemic and hypolipidemic effects (20). Furthermore, CGA is mainly found in *Eucommia ulmoides*, sunflowers, coffee, burdock, honeysuckle and cocoa, and contains a plurality of phenolic hydroxyl groups that form hydrogen radicals and possesses strong antioxidant properties (19). Previous studies have demonstrated that CGA reduces the risk of developing neurodegenerative conditions, such as Alzheimer's and Parkinson's disease, via its inhibitory effect on Aβ40 aggregation (21,23). Additionally, a clinical study has demonstrated that patients who exhibit subjective memory loss of composite and verbal memory show improved complex attention, cognitive flexibility, executive function, motor speed domains of the central nervous system following a 6-month intake of a test beverage containing CGAs prior to bedtime (42). The present study observed that H_2O_2 decreased cell viability and affected the morphology of SH-SY5Y cells. Importantly, CGA ameliorated these morphological alterations and reduced the occurrence of cell apoptosis in a dose- and time-dependent manner following damage by H_2O_2.

To further clarify the mechanism of CGA action in this neuroprotective role, the ALP in H_2O_2-treated SH-SY5Y cells was assessed. The data indicated that CGA treatment reduced the average fluorescence intensity of MDC within the cells and inhibited autophagosome production by downregulating the levels of Beclin-1 and Atg5. Additionally, CGA enhanced lysosomal function in SH-SY5Y cells. Defects of the ALP are strongly associated with AD and the ALP has been reported to regulate APP turnover and Aβ metabolism (43). The accumulation of proinflammatory cytokines and dysfunction of the ALP may damage hippocampal neuronal cells, which is associated with the pathogenesis of AD (44). Autophagy influences the secretion of Aβ to the extracellular space, thereby directly affecting Aβ plaque formation, a pathological hallmark of AD (45). During autophagy, LC3-I is conjugated with phosphatidylethanolamine to form LC3-II, recruited to the autophagosomal membranes and degraded by lysosomal hydrolases following the fusion of autophagosomes with lysosomes (46). Therefore, the LC3-II/I ratio is directly proportional to the number of autophagosomes and is considered to be an important measure of autophagosome levels (46). Cytoplasmic components are selected and tagged prior to being sequestered into

an autophagosome by p62/SQSTM1 during selective autophagy and the transcription of p62 is markedly increased during conditions in which selective autophagy substrates have accumulated (47). Therefore, H_2O_2 treatment induced the levels of LC3-II/I and P62/SQSTM1, while CGA prevented this, preventing the accumulation of autophagic vacuoles and the increase of autophagy-related proteins. Furthermore, defects in lysosomal function appear at the earliest stages of AD development and progress to a widespread failure of intraneuronal waste clearance, neuritic dystrophy and neuronal cell death, as well as inhibition of autophagic flow and decreased levels of autophagosome degradation (48). The results of the present study indicated that CGA enhanced lysosomal function by increasing the levels of CTSD. CTSD upregulation may be an adaptive response to AD-related processes, leading to neurofibrillary degeneration (49). Additionally, the activity of CTSD has been associated with the metabolism of cholesterol and glycosaminoglycans, which accounts for its involvement in neuronal plasticity (50). Therefore, CGA likely serves a vital neuroprotective role during the progression of AD.

The present study aimed to identify the signaling pathway by which CGA affected the progression of AD. TFEB is a transcription factor that upregulates lysosomal function when translocated into the nucleus. mTOR is a key protein involved in regulating factors involved upstream of TFEB nuclear transcription and these factors mainly function to promote TFEB entry into the nucleus by inhibiting phosphorylation of mTOR at the serine 2448 phosphorylation site (51). The results of the present study demonstrated that CGA treatment enhanced the levels of nuclear TFEB and decreased the ratio of P-mTOR/mTOR. It was hypothesized that CGA serves an indispensable neuroprotective role in the process of AD, likely via the mTOR-TFEB signaling pathway. Prior research has revealed that alterations of mTOR signaling and autophagy occur at the early stages of AD and are associated with autophagy impairment (52). Additionally, autophagy is strictly regulated by the mTOR signaling pathway, and regulation of the functional status of autophagy via the mTOR signaling pathway during physical activity is used for the prevention and treatment of AD (53).

In summary, the present study demonstrated that CGA inhibited the activation of the mTOR-TFEB signaling pathway by upregulating lysosomal function and promoting autophagic flux to exert neuroprotective effects.

Acknowledgements

Not applicable.

Funding

The present study was supported by the e National Natural Science Foundation of China (No. 82074150), Key Research and Development Project of Sichuan Province (Major Science and Technology Projects; grant no. 19ZDYF0600) and the Chengdu Technological Innovation R & D project (grant no. 2019-YF05-01332-SN).

Availability of data and materials

The datasets used and/or analyzed during the current study are available from the corresponding author on reasonable request.

Authors' contributions

SJX conceived, designed the experiments and critically revised the manuscript. LJG devised the methodology, performed the experiments and wrote the original draft. XQL performed the data analyses and participated in the revision of the manuscript. YD and ZQZ contributed the sample assays and revised the manuscript. SM performed data analysis and assisted in preparing the figures. All authors read and approved the final manuscript.

Ethics approval and consent to participate

Not applicable.

Patient consent for publication

Not applicable.

Competing interests

The authors declare that they have no competing interests.

References

1. Pugazhenthi S: Metabolic syndrome and the cellular phase of Alzheimer's disease. Prog Mol Biol Transl Sci 146: 243-258, 2017.
2. Ryu JC, Zimmer ER, Rosa-Neto P and Yoon SO: Consequences of metabolic disruption in Alzheimer's disease pathology. Neurotherapeutics 16: 600-610, 2019.
3. Lee M, McGeer E and McGeer PL: Activated human microglia stimulate neuroblastoma cells to upregulate production of beta amyloid protein and tau: Implications for Alzheimer's disease pathogenesis. Neurobiol Aging 36: 42-52, 2015.
4. Hampel H, Mesulam MM, Cuello AC, Khachaturian AS, Vergallo A, Farlow MR, Snyder PJ, Giacobini E and Khachaturian ZS: Revisiting the cholinergic hypothesis in Alzheimer's disease: Emerging evidence from translational and clinical research. J Prev Alzheimers Dis 6: 2-15, 2019.
5. Manyevitch R, Protas M, Scarpiello S, Deliso M, Bass B, Nanajian A, Chang M, Thompson SM, Khoury N, Gonnella R, *et al*: Evaluation of metabolic and synaptic dysfunction hypotheses of Alzheimer's disease (AD): A meta-analysis of CSF markers. Curr Alzheimer Res 15: 164-181, 2018.
6. Haapasalo A, Pikkarainen M and Soininen H: Alzheimer's disease: A report from the 7th Kuopio Alzheimer symposium. Neurodegener Dis Manag 5: 379-382, 2015.
7. Chen XQ and Mobley WC: Exploring the pathogenesis of Alzheimer disease in basal forebrain cholinergic neurons: Converging insights from alternative hypotheses. Front Neurosci 13: 446, 2019.
8. He Z, Guo JL, McBride JD, Narasimhan S, Kim H, Changolkar L, Zhang B, Gathagan RJ, Yue C, Dengler C, *et al*: Amyloid-β plaques enhance Alzheimer's brain tau-seeded pathologies by facilitating neuritic plaque tau aggregation. Nat Med 24: 29-38, 2018.
9. Swomley AM and Butterfield DA: Oxidative stress in Alzheimer disease and mild cognitive impairment: Evidence from human data provided by redox proteomics. Arch Toxicol 89: 1669-1680, 2015.
10. Korovila I, Hugo M, Castro JP, Weber D, Höhn A, Grune T and Jung T: Proteostasis, oxidative stress and aging. Redox Biol 13: 550-567, 2017.
11. Lévy E, El Banna N, Baïlle D, Heneman-Masurel A, Truchet S, Rezaei H, Huang ME, Béringue V, Martin D and Vernis L: Causative links between protein aggregation and oxidative stress: A review. Int J Mol Sci 20: 3896, 2019.
12. Chu Q, Zhu Y, Cao T, Zhang Y, Chang Z, Liu Y, Lu J and Zhang Y: Studies on the neuroprotection of osthole on glutamate-induced apoptotic cells and an Alzheimer's disease mouse model via modulation oxidative stress. Appl Biochem Biotechnol 190: 634-644, 2020.

13. Alvariño R, Alonso E, Abbasov ME, Chaheine CM, Conner ML, Romo D, Alfonso A and Botana LM: Gracilin A derivatives target early events in Alzheimer's disease: In vitro effects on neuroinflammation and oxidative stress. ACS Chem Neurosci 10: 4102-4111, 2019.
14. Bagherniya M, Butler AE, Barreto GE and Sahebkar A: The effect of fasting or calorie restriction on autophagy induction: A review of the literature. Ageing Res Rev 47: 183-197, 2018.
15. Castillo K, Valenzuela V, Oñate M and Hetz C: A molecular reporter for monitoring autophagic flux in nervous system in vivo. Methods Enzymol 588: 109-131, 2017.
16. Reddy PH and Oliver DM: Amyloid beta and phosphorylated tau-induced defective autophagy and mitophagy in Alzheimer's disease. Cells 8: 488, 2019.
17. Correia SC, Resende R, Moreira PI and Pereira CM: Alzheimer's disease-related misfolded proteins and dysfunctional organelles on autophagy menu. DNA Cell Biol 34: 261-273, 2015.
18. Damme M, Suntio T, Saftig P and Eskelinen EL: Autophagy in neuronal cells: General principles and physiological and pathological functions. Acta Neuropathol 129: 337-362, 2015.
19. Gao L, Li X, Meng S, Ma T, Wan L and Xu S: Chlorogenic acid alleviates $A\beta_{25-35}$-induced autophagy and cognitive impairment via the mTOR/TFEB signaling pathway. Drug Des Devel Ther 14: 1705-1716, 2020.
20. Farhood HB, Balas M, Gradinaru D, Margina D and Dinischiotu A: Hepatoprotective effects of chlorogenic acid under hyperglycemic conditions. Rom Biotechnol Lett: 1-10, 2017.
21. Heitman E and Ingram DK: Cognitive and neuroprotective effects of chlorogenic acid. Nutr Neurosci 20: 32-39, 2017.
22. Tajik N, Tajik M, Mack I and Enck P: The potential effects of chlorogenic acid, the main phenolic components in coffee, on health: A comprehensive review of the literature. Eur J Nutr 56: 2215-2244, 2017.
23. Yang L, Wang N and Zheng G: Enhanced effect of combining chlorogenic acid on selenium nanoparticles in inhibiting amyloid β aggregation and reactive oxygen species formation in vitro. Nanoscale Res Lett 13: 303, 2018.
24. Taram F, Winter AN and Linseman DA: Neuroprotection comparison of chlorogenic acid and its metabolites against mechanistically distinct cell death-inducing agents in cultured cerebellar granule neurons. Brain Res 1648: 69-80, 2016.
25. Wang XJ, Wang LY, Fu Y, Wu J, Tang XC, Zhao WM and Zhang HY: Promising effects on ameliorating mitochondrial function and enhancing Akt signaling in SH-SY5Y cells by (M)-bicelaphanol A, a novel dimeric podocarpane type trinorditerpene isolated from Celastrus orbiculatus. Phytomedicine 20: 1064-1070, 2013.
26. Zheng Y, Ma L, Liu N, Tang X, Guo S, Zhang B and Jiang Z: Autophagy and apoptosis of porcine ovarian granulosa cells during follicular development. Animals (Basel) 9: 1111, 2019.
27. Shi C, Zhao L, Zhu B, Li Q, Yew DT, Yao Z and Xu J: Dosage effects of EGb761 on hydrogen peroxide-induced cell death in SH-SY5Y cells. Chem Biol Interact 180: 389-397, 2009.
28. Wang W, Sun F, An Y, Ai H, Zhang L, Huang W and Li L: Morroniside protects human neuroblastoma SH-SY5Y cells against hydrogen peroxide-induced cytotoxicity. Eur J Pharmacol 613: 19-23, 2009.
29. Yu BW, Li JL, Guo BB, Fan HM, Zhao WM and Wang HY: Chlorogenic acid analogues from Gynura nepalensis protect H9c2 cardiomyoblasts against H_2O_2-induced apoptosis. Acta Pharmacol Sin 37: 1413-1422, 2016.
30. Chao X, Ni HM and Ding WX: Insufficient autophagy: A novel autophagic flux scenario uncovered by impaired liver TFEB-mediated lysosomal biogenesis from chronic alcohol-drinking mice. Autophagy 14: 1646-1648, 2018.
31. Aghdaei HA, Kadijani AA, Sorrentino D, Mirzaei A, Shahrokh S, Balaii H, Geraci M and Zali MR: An increased Bax/Bcl-2 ratio in circulating inflammatory cells predicts primary response to infliximab in inflammatory bowel disease patients. United European Gastroenterol J 6: 1074-1081, 2018.
32. Zhao T, Fu Y, Sun H and Liu X: Ligustrazine suppresses neuron apoptosis via the Bax/Bcl-2 and caspase-3 pathway in PC12 cells and in rats with vascular dementia. IUBMB Life 70: 60-70, 2018.
33. Katsuragi Y, Ichimura Y and Komatsu M: p62/SQSTM1 functions as a signaling hub and an autophagy adaptor. FEBS J 282: 4672-4678, 2015.
34. Ahsan A, Zheng Y, Ma S, Liu M, Cao M, Li Y, Zheng W, Zhou X, Xin M, Hu WW, *et al*: Tomatidine protects against ischemic neuronal injury by improving lysosomal function. Eur J Pharmacol 882: 173280, 2020.
35. Schaaf MB, Houbaert D, Meçe O, To SK, Ganne M, Maes H and Agostinis P: Lysosomal pathways and autophagy distinctively control endothelial cell behavior to affect tumor vasculature. Front Oncol 9: 171, 2019.
36. Pierzyńska-Mach A, Janowski PA and Dobrucki JW: Evaluation of acridine orange, LysoTracker Red, and quinacrine as fluorescent probes for long-term tracking of acidic vesicles. Cytometry A 85: 729-737, 2014.
37. Thapa A and Carroll NJ: Dietary modulation of oxidative stress in Alzheimer's disease. Int J Mol Sci 18: 1583, 2017.
38. Pohanka M: Alzheimer's disease and oxidative stress: A review. Curr Med Chem 21: 356-364, 2014.
39. Gubandru M, Margina D, Tsitsimpikou C, Goutzourelas N, Tsarouhas K, Ilie M, Tsatsakis AM and Kouretas D: Alzheimer's disease treated patients showed different patterns for oxidative stress and inflammation markers. Food Chem Toxicol 61: 209-214, 2013.
40. Lee HJ, Spandidos DA, Tsatsakis A, Margina D, Izotov BN and Yang SH: Neuroprotective effects of Scrophularia buergeriana extract against glutamate-induced toxicity in SH-SY5Y cells. Int J Mol Med 43: 2144-2152, 2019.
41. Costa C, Tsatsakis A, Mamoulakis C, Teodoro M, Briguglio G, Caruso E, Tsoukalas D, Margina D, Dardiotis E, Kouretas D and Fenga C: Current evidence on the effect of dietary polyphenols intake on chronic diseases. Food Chem Toxicol 110: 286-299, 2017.
42. Kato M, Ochiai R, Kozuma K, Sato H and Katsuragi Y: Effect of chlorogenic acid intake on cognitive function in the elderly: A pilot study. Evid Based Complement Alternat Med 2018: 8608497, 2018.
43. Martini-Stoica H, Xu Y, Ballabio A and Zheng H: The autophagy-lysosomal pathway in neurodegeneration: A TFEB perspective. Trends Neurosci 39: 221-234, 2016.
44. Wang D, Zhang J, Jiang W, Cao Z, Zhao F, Cai T, Aschner M and Luo W: The role of NLRP3-CASP1 in inflammasome-mediated neuroinflammation and autophagy dysfunction in manganese-induced, hippocampal-dependent impairment of learning and memory ability. Autophagy 13: 914-927, 2017.
45. Ntsapi C, Lumkwana D, Swart C, du Toit A and Loos B: New insights into autophagy dysfunction related to amyloid beta toxicity and neuropathology in Alzheimer's disease. Int Rev Cell Mol Biol 336: 321-361, 2018.
46. Tanida I and Waguri S: Measurement of autophagy in cells and tissues. Methods Mol Biol 648: 193-214, 2010.
47. Lamark T, Svenning S and Johansen T: Regulation of selective autophagy: The p62/SQSTM1 paradigm. Essays Biochem 61: 609-624, 2017.
48. Colacurcio DJ, Pensalfini A, Jiang Y and Nixon RA: Dysfunction of autophagy and endosomal-lysosomal pathways: Roles in pathogenesis of down syndrome and Alzheimer's disease. Free Radic Biol Med 114: 40-51, 2018.
49. Chai YL, Chong JR, Weng J, Howlett D, Halsey A, Lee JH, Attems J, Aarsland D, Francis PT, Chen CP and Lai MKP: Lysosomal cathepsin D is upregulated in Alzheimer's disease neocortex and may be a marker for neurofibrillary degeneration. Brain Pathol 29: 63-74, 2019.
50. Vidoni C, Follo C, Savino M, Melone MA and Isidoro C: The role of cathepsin D in the pathogenesis of human neurodegenerative disorders. Med Res Rev 36: 845-870, 2016.
51. Ye B, Wang Q, Hu H, Shen Y, Fan C, Chen P, Ma Y, Wu H and Xiang M: Restoring autophagic flux attenuates cochlear spiral ganglion neuron degeneration by promoting TFEB nuclear translocation via inhibiting MTOR. Autophagy 15: 998-1016, 2019.
52. Tramutola A, Triplett JC, Di Domenico F, Niedowicz DM, Murphy MP, Coccia R, Perluigi M and Butterfield DA: Alteration of mTOR signaling occurs early in the progression of Alzheimer disease (AD): Analysis of brain from subjects with pre-clinical AD, amnestic mild cognitive impairment and late-stage AD. J Neurochem 133: 739-749, 2015.
53. Kou X, Chen D and Chen N: Physical activity alleviates cognitive dysfunction of Alzheimer's disease through regulating the mTOR signaling pathway. Int J Mol Sci 20: 1591, 2019.